ISSN (print): 1698-6180. ISSN (online): 1886-7995
www.ucm.es/info/estratig/journal.htm

Journal of Iberian Geology 35 (1) 2009: 5-18

Determination of seismogenic structures and earthquake magnitud from seismites in the Acequion river, Precordillera Range, central-western Argentina

Determinación de las estructuras sismogénicas y la magnitud del terremoto a partir de sismitas en el río Acequión, Precordillera, centro-oeste argentino

L. P. Perucca*[1,2], A. I. Bracco[3], S. M. Moreiras[1,4]

[1]Consejo Nacional de Investigaciones Científicas y Tecnológicas (CONICET), Argentina
[2] Gabinete de Neotectónica. INGEO. Facultad de Ciencias Exactas, Físicas y Naturales. Universidad Nacional de San Juan, Argentina. e-mail: lperucca@unsj-cuim.edu.ar
[3]Gabinete de Estratigrafía. INGEO. Facultad de Ciencias Exactas, Físicas y Naturales. Universidad Nacional de San Juan, Argentina. e-mail: adrygeo@yahoo.com.ar
[4]Instituto Argentino de Nivología, Glaciología y Ciencias Ambientales (IANIGLA) - CRICYT, Argentina. e-mail: moreiras@lab.cricyt.edu.ar
**Corresponding autor: L.P. Perucca*

Received: 20/03/07 / Accepted: 30/11/07

Abstract

Evidences for paleoearthquake induced liquefaction features in the Central Western Argentina were determined in the Acequión river valley. Well-preserved liquefaction structures were found in a Holocene lake dammed by rock avalanches. At least five paleoearthquakes affected this region during the Pleistocene-Holocene according to the temporal sequence established for these seismic structures and the rock avalanches recognized in the Acequion river. The magnitude of these triggering paleoevents and probable seismic source are analysed and discussed, concluding that liquefaction features and rock avalanches should be generated by M>5 earthquakes related to the nearby Cerro Salinas Fault belonging to Precordillera Oriental fault system. These findings allow us to extend the record of moderate to high magnitude-earthquakes to the Pleistocene-Holocene.

Keywords: lacustrine, liquefaction, rock avalanches, earthquake magnitude, Cerro Salinas Fault, Precordillera Argentina

Resumen

Se reconocieron en la quebrada del río Acequión ubicada en la región centro-oeste de la Argentina, numerosas evidencias de la ocurrencia de paleoterremotos generadores de estructuras de licuefacción y fenómenos de remoción en masa. Estas estructuras de licuefacción se ubicaron en un lago de edad Holocena originado por una avalancha de rocas. Según la sucesión temporal establecida para estas estructuras sísmicas y asumiendo un origen sísmico para la avalancha de rocas, por lo menos cinco paleoterremotos habrían afectado esta región durante el Pleistoceno-Holoceno.

Se discute además, la magnitud de estos paleoeventos y la probable fuente sismogénica, concluyendo que las estructuras de licuefacción y las avalanchas de roca deben haberse generado por terremotos de M>5 relacionados a la falla del Cerro Salinas, ubicada a escasos kilómetros al oeste, la cual pertenece al sistema de fallamiento Precordillera Oriental.

Los resultados obtenidos en esta porción del territorio argentino, permiten extender el registro de terremotos de magnitud moderada a alta, al Pleistoceno-Holoceno.

Palabras clave: lacustre, licuefacción, avalancha de roca, magnitud del terremoto, falla del Cerro Salinas, Precordillera Argentina.

1. Introduction

The active seismicity of the Andean backarc in the Central Western Argentina is related to the Pampean flat-slab segment of the Nazca Plate (between 28ºS and 33ºS) (Stern, 2004), whose activity initiated 8-10 My ago (Fig. 1a) (Jordan and Gardeweg, 1987; Kay *et al*., 1991). Central-Western Argentina region is characterised by an intense shallow seismic activity (5 to 50 km in depth) (Smalley and Isacks, 1990; Suarez *et al*., 1983), but a moderate to high activity also exits between 90 and 150 km (INPRES, 1993) (Fig. 1b). According to Costa *et al*. (2000), 80% of Quaternary deformation in the Argentina is concentrated in this region.

Central Western Argentina, comprising San Juan and Mendoza provinces, which capital cities are located 300 km eastern of the convergence boundary, has been affected by at least 8 destructive earthquakes (Ms≥6.3) during the last 300 years (Fig. 1c). These earthquakes caused the most severe damages and secondary effects such as landslides and liquefaction phenomena (Bodenbender, 1894; Harrington, 1944; Loos, 1926, 1928; Lünkenheimer, 1929; Moreiras, 2006, Perucca and Moreiras, 2006).

The paleoseismicity of a region can be analysed recognising the earthquake-induced effects preserved through the geological record and applying empirical relations based on extension of surface rupture or displacement (Obermeier *et al*. 2001). In this study, both methods were carried out on liquefaction features identified in two Quaternary (Pleistocene-Holocene) paleolake sequences resulting from the damming of the Acequión river due two ancient rock avalanches. Deformation structures occur close to an active Quaternary fault system located in the nearness. Determination of both earthquake magnitude and possible seismogenic structures have been carried out from the study of these soft-sediment deformation structures here interpreted as seismites.

2. Tectonic setting

The Acequión river valley is located 120 km south of San Juan City (San Juan province, Argentina) at 32º 15' S and 68º 45' W in Central-Western Argentina (Fig. 2a). The Acequión river is a permanent stream that crosses with a SE direction the Cambro-Ordovician calcareous rocks of the Sierra de Pedernal. This range represents the southern portion of the Precordillera Oriental geological province which is considered a long, west verging thin skinned fold-thrust belt in which Paleozoic, Triassic and Cenozoic rocks form the eastern foothills of the Andean Cordillera (Fig. 2b).

The Precordillera Oriental geological province has an asymmetric profile, with a narrower and steeper flank on the western border, and a moderate eastern flank with extended slopes (Fig. 2c). This asymmetric profile is also observed in both piedmonts. The western one is 2 km wide with slopes between 20º and 25º, while the eastern one is 10 km wide with slopes between 5º and 7º (Bastias *et al*., 1990, Martos, 1999, Perucca and Paredes, 2004). Although it is possible to recognize geomorphologic features such as antislope scarps in both piedmonts, the current preservation of these features and the number of faults is quite different. While in the western foothills the scarps are scarce, discontinuous and affect only Pleistocene deposits, in the eastern piedmont the scarps are parallel and face to the West, affecting different alluvial fans, pediment levels, and Holocene fluvial terraces (Fig. 2c). These faults stretching for approximately 150 km along a North-South trend is known as *Precordillera Oriental* fault system, an east dipping reverse fault system composed of several fault segments (Ortiz and Zambrano, 1981). This fault system was the responsible of the earthquake of January 15th 1944 (Ms 7.4). This seismic shock is considered the most significant natural disaster in Argentine history (see Figure 1c).

The Cerro Salinas fault, belonging to the *Precordillera Oriental* fault system, is a fault zone consisting on several faults segments affecting the western flank of an anticline (Ramos *et al*., 1997). This fault zone exposes the westernmost outcrops of the *Sierras Pampeanas* basement at this latitude. This fault zone defines the boundary between the Pampean broken foreland and the *Precordillera* fold-thrust belt. Ortiz *et al*. (1975) noted that this fault zone is a Precambrian basement rock core thrusting over Quaternary deposits.

Vergés *et al*., (2002) mentioned the Cerro Salinas structure, formed by a monocline front developed above a West vergent - East deeping crustal ramp, begun its activ-

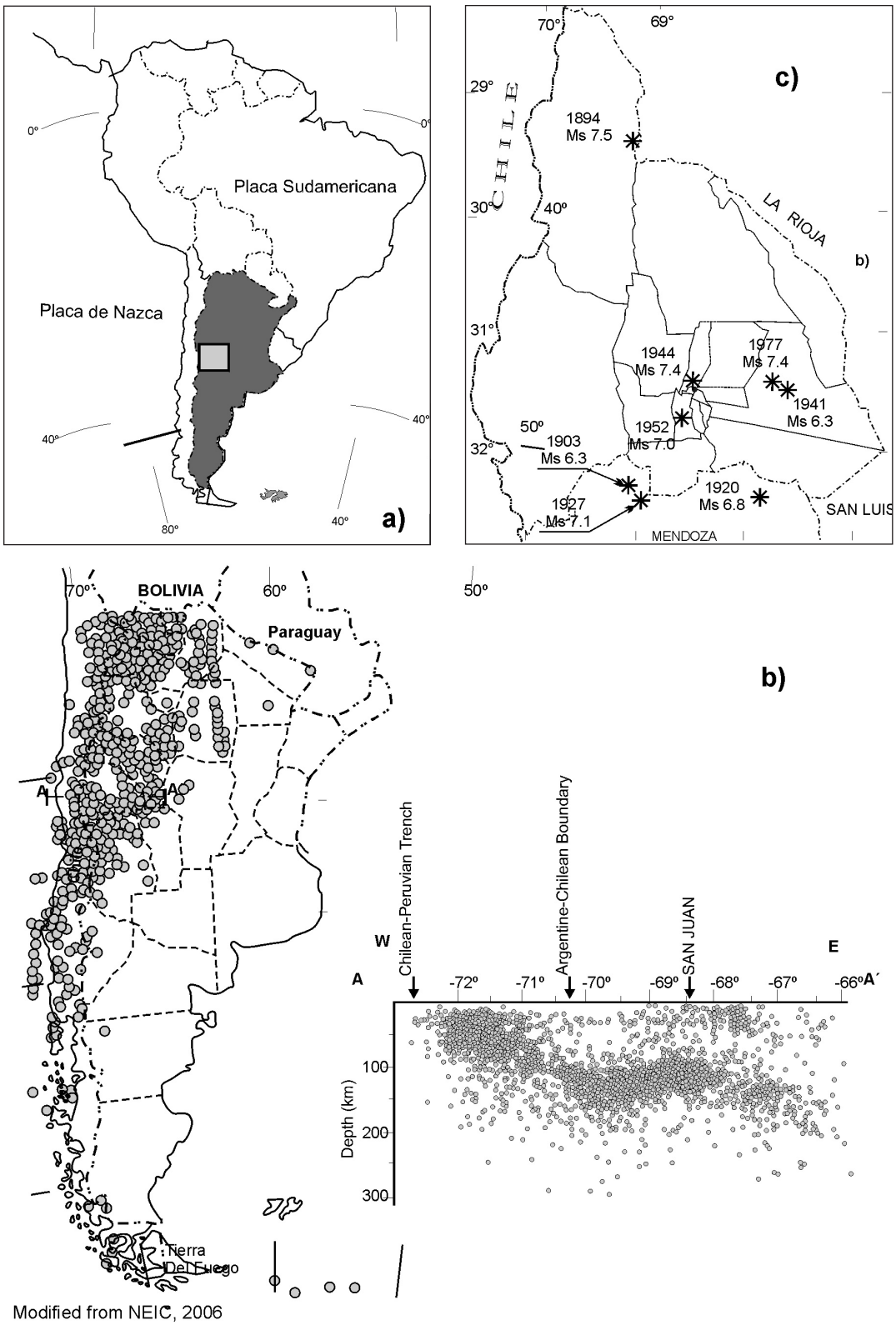

Fig. 1.- a) Geographical location map of the studied area and the Nazca and South American plates. b) Seismicity of Argentine, Ms>5 earthquakes since 1973 (Depth 0-30 km) (Modified from NEIC, 2006) and West- East seismic cross-section (A-A') between 28° and 33º 30' SL (Modified from INPRES, 1993). c) Main historical earthquakes (Ms≥6.3) in the study area neighboring

Fig. 1.- a) Mapa de ubicación del área de estudio y de las placas Nazca y Sudamericana. b) Sismicidad de la Argentina, terremotos de magnitud M>5 desde 1973 (Profundidad 0-30km) (Modificado de NEIC, 2006) y perfil sísmico transversal Oeste-Este (A-A') entre los 28º y 33º 30'LS (Modificado de INPRES, 1993). c) Principales terremotos históricos (Ms≥6.3) ocurridos en la región

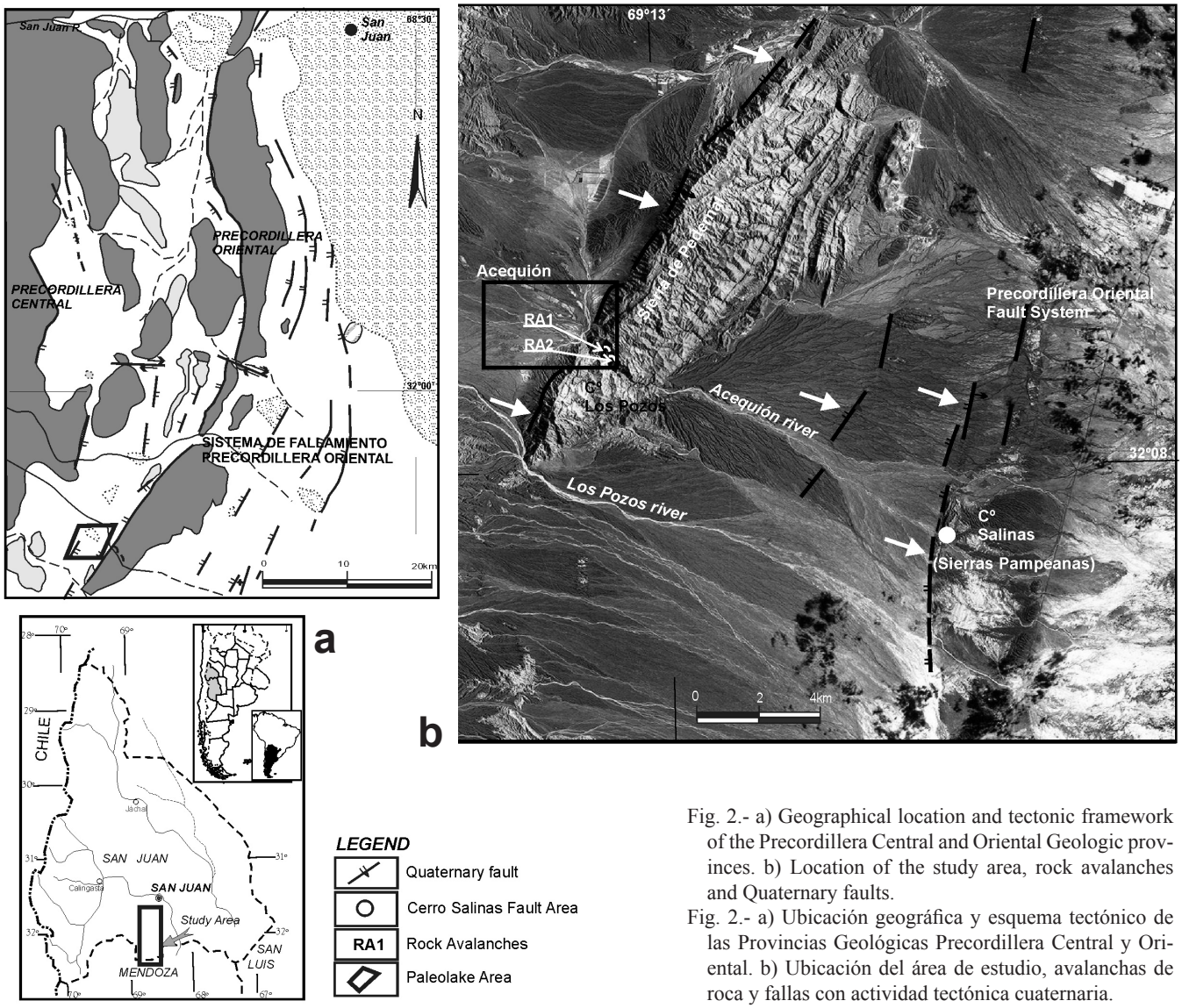

Fig. 2.- a) Geographical location and tectonic framework of the Precordillera Central and Oriental Geologic provinces. b) Location of the study area, rock avalanches and Quaternary faults.

Fig. 2.- a) Ubicación geográfica y esquema tectónico de las Provincias Geológicas Precordillera Central y Oriental. b) Ubicación del área de estudio, avalanchas de roca y fallas con actividad tectónica cuaternaria.

ity during the Late Miocene continuing until very recent times indicated by various faulted and folded alluvial terraces. Martos (2002) working on these deposits settled on at least four reactivations of the Cerro Salinas fault system during the Holocene with a mean recurrence of 2500 years. This author also determined the probably maximum magnitude of these earthquakes was Ms 6.7. Most recent activity of this system fault was related to the Ms 7 earthquake occurred on June 10th 1952, although no evidence of surface rupture had been found (Tello and Perucca, 1993). After this earthquake, several secondary effects like fissures, liquefaction phenomena, and landslides were identified in nearby areas to the epicentre.

According to mentioned above, the active Cerro Salinas fault zone, located 18 km Eastern of the study area, is the most likely source area, for at least 3 of the 5 paleoearthquakes established in this study.

3. Liquefaction features and rock avalanches

Two rock avalanches dammed the Acequión river causing associated lakes. The older paleolake had an extension of 6 km^2; whereas the younger covered a smaller area (Fig. 3). In the former, the water level reached to 1,250 m a.s.l. in altitude and its lacustrine sequence has 25 m in thickness (Fig. 4a). Organic matter (especially plants) collected in the basal levels of the paleolake was radiocarbon dated in 15,540 ±370 ^{14}C BP and a piece of wood found in the basal levels of the younger paleolake related to RA-2 rock avalanche was radiocarbon dated too given an age of 7,497±157 ^{14}C BP.

Both paleolake sequences are constituted by brownish fine grained sediments where sand - clay levels are intercalated. The sediments of the younger paleolake, that reached an altitude of 1200 m a.s.l. (Fig. 4a), are well

Fig. 3.- Schematic map of the Acequión area showing inferred borders of paleo-lakes, distribution of liquefaction features, and location of rock avalanches.

Fig. 3.- Mapa esquemático del area Acequión mostrando los límites inferidos de los paleolagos, la distribución de las estructuras de licuefacción y la ubicación de las avalanchas de roca.

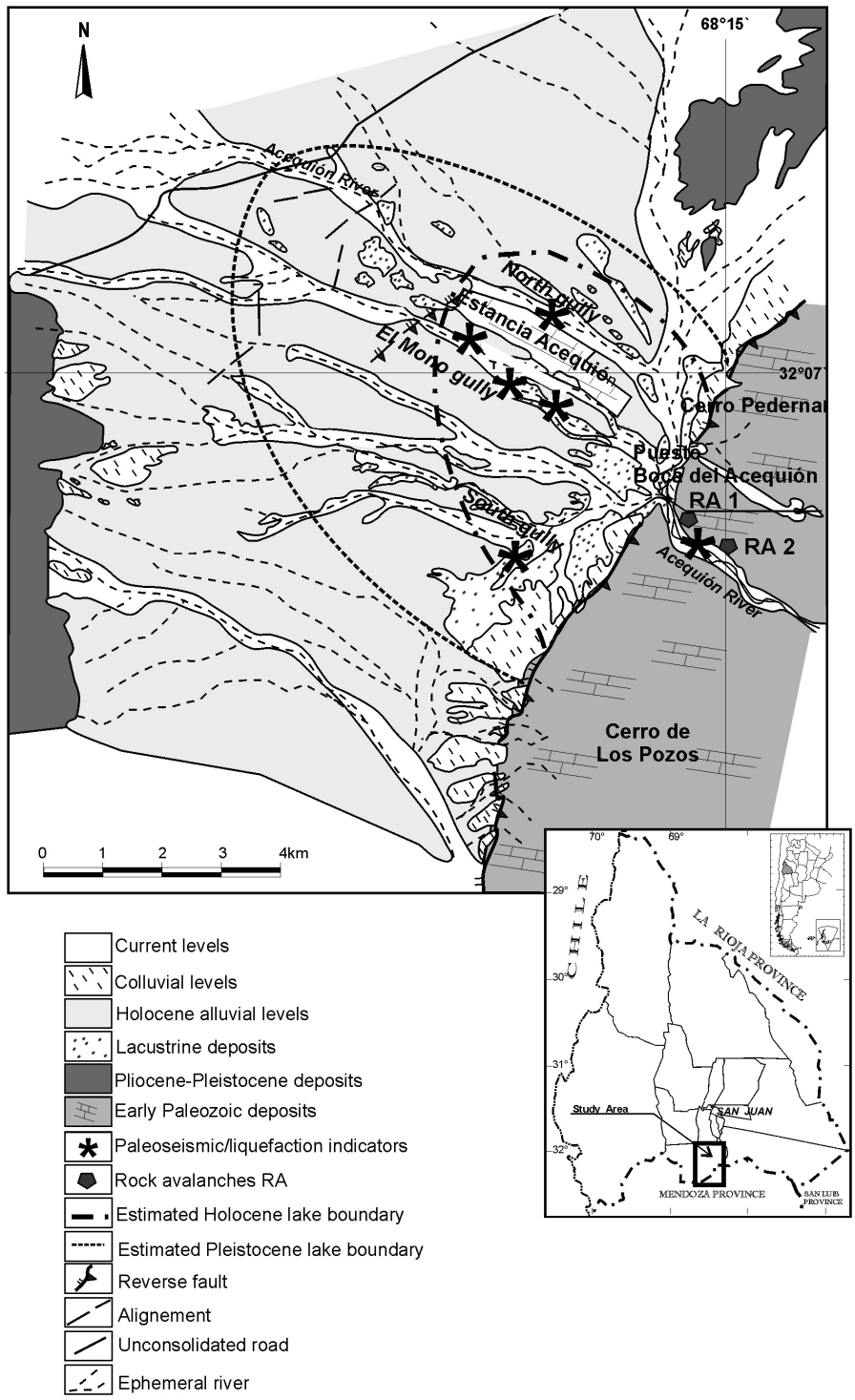

exposed in the El Mono gully. They consist of poorly consolidated sandstones and alternating silt-clayed layers with a total thickness of 10 m. The sandy layers are thicker on the west side of the El Mono and South gullies, whilst towards the East interbedded clay, silt and thin calcareous layers predominate (Fig. 4b).

Deformed lacustrine deposits of Holocene paleolake are covered by gravels (Paredes and Perucca, 2000) which have been correlated along the studied area. This alluvial sequence constitutes the limit between both lakes.

Many liquefaction features were observed along the creeks eroded within the sediments of the Holocene paleolake related to the RA-2 rock avalanche. These structures, initially mentioned by Paredes and Perucca (2000), are described in detail in this study regarding their main characteristics and distribution.

Sand dikes and diapirs were identified at several levels of the stratigraphic succession of the lacustrine sediments

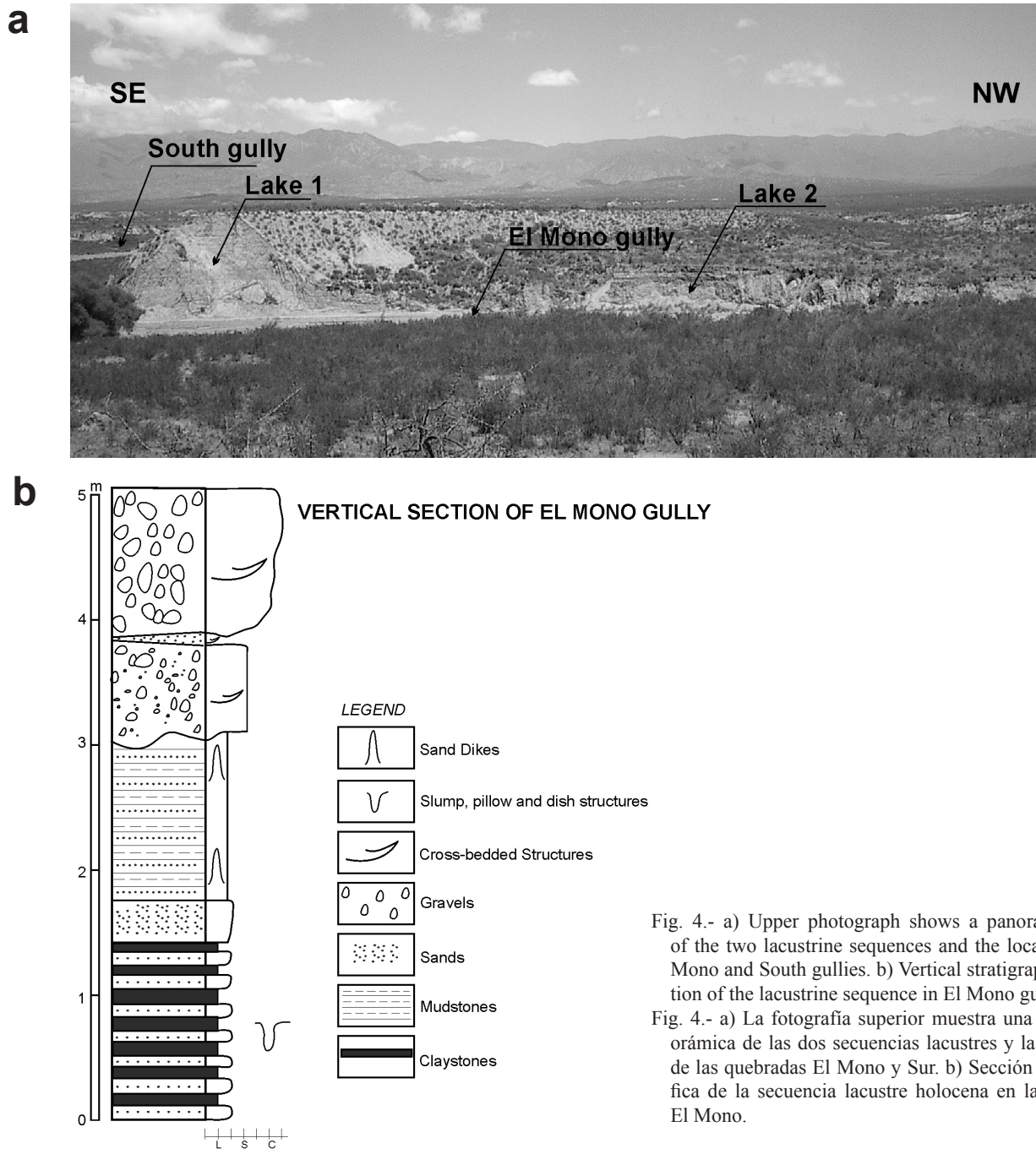

Fig. 4.- a) Upper photograph shows a panoramic view of the two lacustrine sequences and the location of El Mono and South gullies. b) Vertical stratigraphical section of the lacustrine sequence in El Mono gully.

Fig. 4.- a) La fotografía superior muestra una vista panorámica de las dos secuencias lacustres y la ubicación de las quebradas El Mono y Sur. b) Sección estratigráfica de la secuencia lacustre holocena en la quebrada El Mono.

related to RA-2 rock avalanches, particularly in the El Mono creek (Fig. 5 a,b). A network of dikes made up of large sand intrusions linked with small ones is frequently observed. The upward motion of sand is supported by the fact that major dikes are rooted in a basal sand bed and contiguous confining layers show upward bending.

In general, these sand dikes have irregular form, from 1m to 4 m thick and up to 4 m high. Figure 6 shows one of the larger sand dikes, in which a 3.6 m wide feeder channel and areas of accumulation of angular clasts originated from sidewall material (silty-clay) are visible. The clastic material is oriented in an upward direction, parallel to the border. Towards the top of the structure, a cap composed by gravel and sand is visible, accompanied by smaller sand dikes of similar characteristics and faults.

Due to the low cohesion of the injected material, frequent collapses along liquefaction structures are observed along the creeks. In some cases, only the mould of the feeding channel and cone has remained.

The thickness of the sand dikes decreases toward the East of the El Mono gully, where the thickest sand dikes (less than 0,1m wide) were found.

Several sand injection structures combined with sills, slumps, and faults are recognized too. As Figure 5a shows,

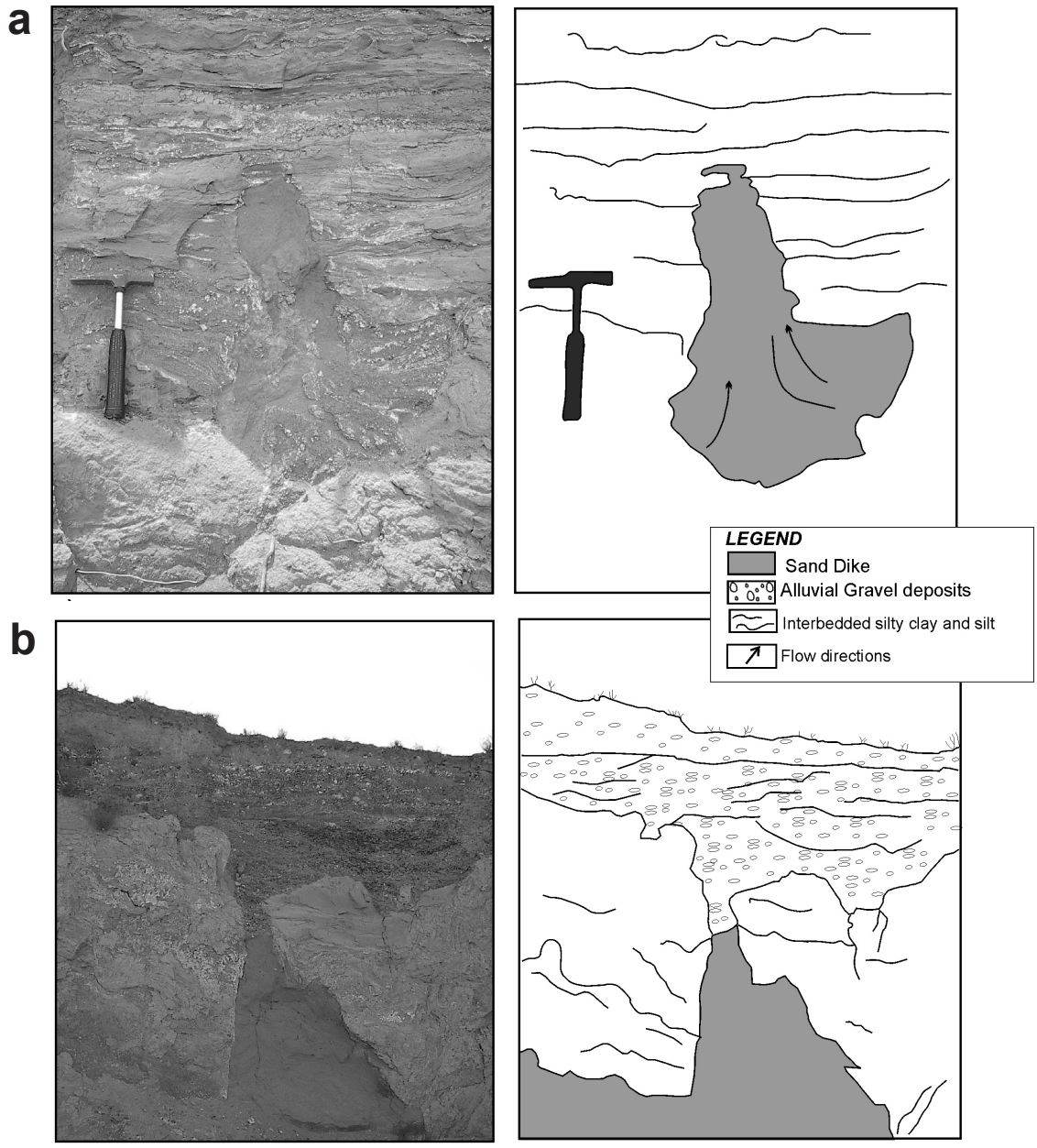

Fig. 5.- Photographs and schemes in El Mono gully showing some liquefaction features.- a - sand diapir and slumps, b.- Sand dike affecting the upper level of alluvial gavels.

Fig. 5.- Fotografías y esquemas en la quebrada El Mono que muestran algunas estructuras de licuefacción. a- Domo diapírico de arena y estructuras en slump, b- Dique de arena que afecta el nivel superior de gravas aluviales

the sand injections look like diapiric domes, sometimes rounded and some others conical. The sand is not very cohesive, with mid-size well classified grains. No internal structures can be identified and contacts with the sidewall are mostly irregular. In the lower section of the intrusion, there is a high concentration of clasts with sizes ranging from 30 cm to 40 cm long and 15 cm wide.

Several lacustrine levels display disrupted lamination and other kinds of convolute bedding forming recumbent or isoclinal folds along the El Mono gully. The upper contact of these layers with the overlying strata is nearly flat, indicating that the internal flow within the sand layer caused convolutions. Towards the top of the sequence, dish structures were observed with irregular, rounded calcareous nodules floating in a sand matrix (Fig. 7).

Paredes and Perucca (2000) recognized numerous liquefaction features like sand dikes in a natural trench located in El Mono gully (Fig. 8a). They observed too a vertical thin sand dike that intrudes a deposit of interbedded silty clay and silty sand in the South gully (Fig. 8b). The dike is about 10 cm wide and it is composed of fine sand and silt.

Three clastic dikes filled with mud (Fig. 3) were recognized between the two rock avalanches, The fill material is homogeneous in composition and the dikes range in thickness from about 5 to 7 cm and in length from 2 to 4m. The dikes are tabular and nearly vertical.

Lake deposits are also cut by numerous faults, most of them normal. The faults have variable orientations, but they strike generally north-south and dip to the west and

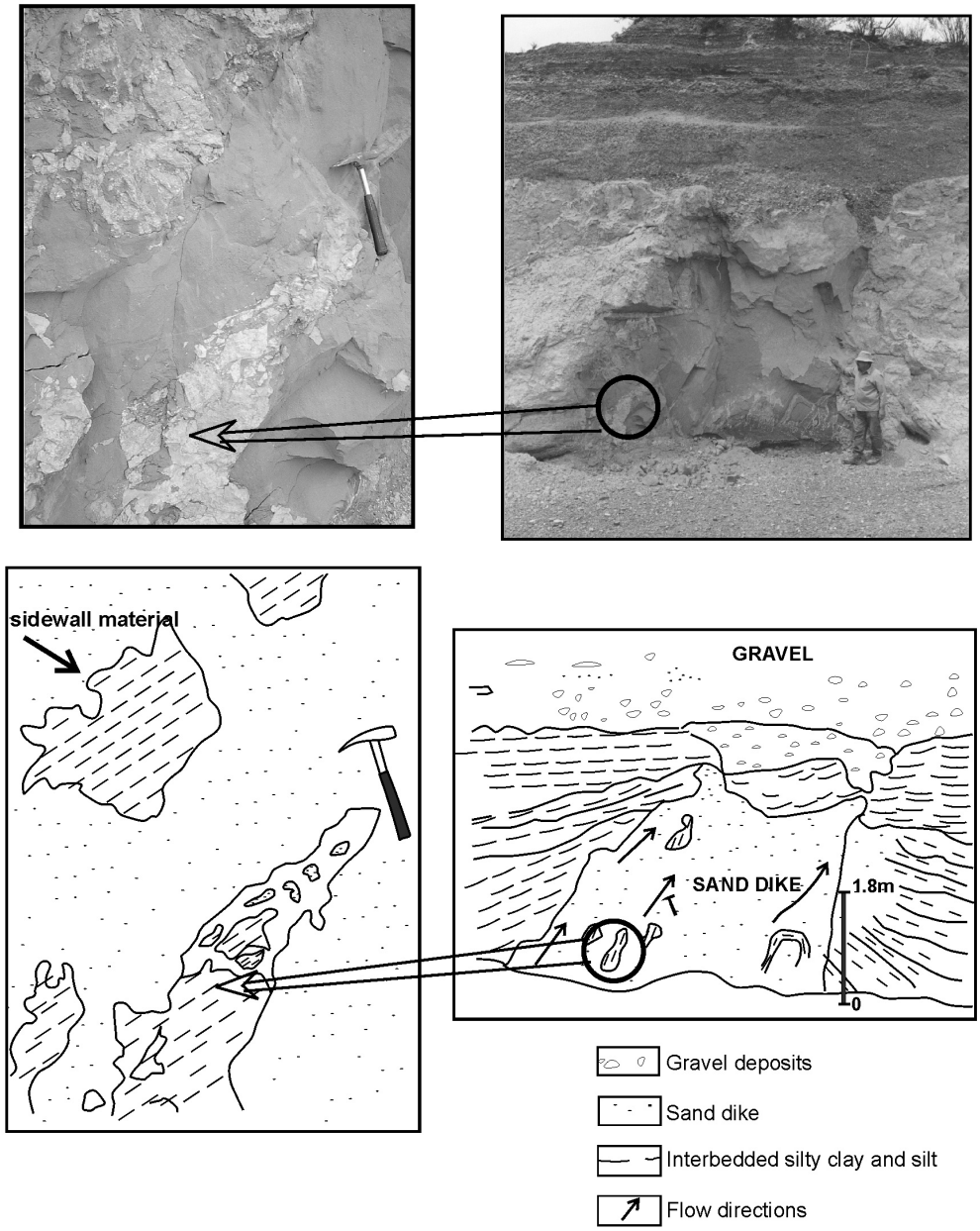

Fig. 6.- Photograph and scheme of the thick sand dike containing clasts of sidewall material (silt-clay) observed in the El Mono gully. The upper level of gravel material is disturbed too. The liquefied sand layer shows flow structures indicating upward injection of sand-filled clastic dike.

Fig. 6.- Fotografía y esquema del dique ancho observado en la quebrada El Mono. El dique contiene clastos del material de la roca encajante (limoarcillosa). El nivel superior constituido por gravas aluviales también está disturbado. La capa de arena licuefactada muestra estructuras de flujo que indican la inyección del material arenoso hacia arriba.

east alternatively. The dip-slip displacement on the faults ranges from a few centimeters to 1m.

4. Spatial distribution and probable sequence of liquefaction structures

Even through, sand dikes are broadly spread out in Holocene lake sediments related to RA-2 rock avalanche, the most spectacular structures are found along the El Mono gully. The width of these structures is variable from 10 cm to 4 m wide, anyway the thinner ones predominate. Moreover, sand dikes width and their quantity increase toward the East; they are particularly abundant and thicker near the Boca del Acequión place. Other deformation structures identified in this Holocene lake sequence, such as large domes, dishes, joints, and sand-filled fissures, also increase in size towards East. It is notable that liquefaction structures were not found in the west sector of this paleolake, neither in northern and southern gullies eroded on these deposits. These observations suggest that the seismic source may have been located in that direction because sand dikes become thinner with greater distance from the epicentre (Munson *et al*., 1995; Obermeier, 1998).

Moreover, Paredes and Perucca (2000) analysing the relationships among sand dikes identified along the El Mono and South gullies, thus establishing the temporal sequence of these liquefaction features, determined at least three paleoearthquakes. The first paleoearthquake is related to a dike called *Oriental dike* (Fig. 8 a) that was

subsequently intruded, and tilted, by another dike called *Occidental dike* that should be linked to a latter seismic event. It was note that thicker strata overlaying lake sediments were not affected by these structures. These structures were located in the El Mono gully.

A new paleoearthquake may have caused the so-called Narrow Dike, situated in the South gully, which cut across the two previous sequences present in the area and a cyneritc level indicating a third paleoevent later to the alluvial conglomerate depositation (Fig. 8b). Relationship among these sand dikes studied in this paper, correlates well with findings from previous works.

Temporal sequence for further structures could not be determined because they are not always in contact or in a clear relation as the case presented above.

5. Paleoearthquake magnitude estimation

The aim of this study was to determine the characteristics of paleoearthquakes related to liquefaction features identified in two quaternary paleolake sequences resulting from the dam of the Acequion river by two ancient rock avalanches.

Several exposed profiles resulting from the erosion of lacustrine sequences were studied in detail for identification of liquefaction structures and faults. Analysing these features interrelations, a sequence of paleoearthquakes was determined.

It is usually assumed that the size and spatial distribution of liquefaction features reflect the source region of a paleoearthquake and the regional distribution of similar-age features is thought to represent the area where strong ground shaking would be felt and the largest liquefaction features define the epicentral area of a paleoearthquake (Tuttle, 2001).

Moreover, the width of sand dikes was analysed for determining the probable seismic source of this paleoearthquakes, as it is known that sand dikes become thinner as the distance from the epicentre increases. For example, the range of liquefaction effects originated during the 1886 Charleston earthquake (Ms 7.2) was used in combination with the sizes of liquefaction features to demonstrate that previous events had been at least as strong as that of 1886 (Obermeier, 1996). In the Wabash Valley of Indiana Illinois, Munson *et al*., (1995) and Obermeier, (1998) used these relationships to demonstrate that some of the prehistoric earthquakes occurred in this region exceeded Ms 7.

Furthermore, magnitude of these triggering pre-historic earthquakes was estimated by different methods what vary widely in their basic approaches, thus allow an independent assessment. The earthquake magnitude has been

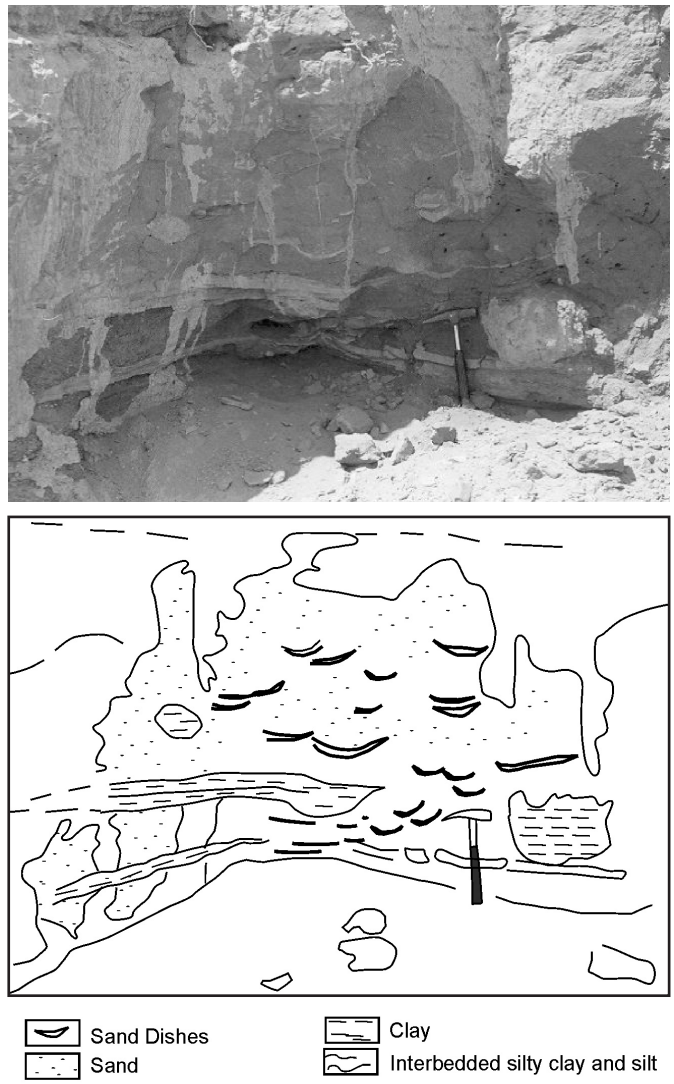

Fig. 7.- Photograph and scheme showing silt and clay nodules and dish structures within a sand matrix. The natural trench is located in the North gully.

Fig. 7.- Fotografía y esquema mostrando nódulos de limo y arcilla dentro de una matriz arenosa. La trinchera natural se localiza en la quebrada norte.

estimated using the *magnitude bound method* based on the relationship between earthquake moment magnitude and the farthest distance from the seismic source to the liquefaction zone. This was carried out assuming that seismic source was the Cerro Salinas fault related to Precordillera Oriental fault system because this one affects Holocene deposits. Equations established by Allen (1986) (eq. 1) and Ambraseys (1988) (eq. 2) were considered. These authors determined the relationship between maximum epicentral distance (Re) between epicentre and liquefaction features analysing earthquake-triggered liquefaction structures around the world. Initially, Allen (1986) using the empirical relationships established by Kuribayashi and Tatsuoka (1975) derived the following equation:

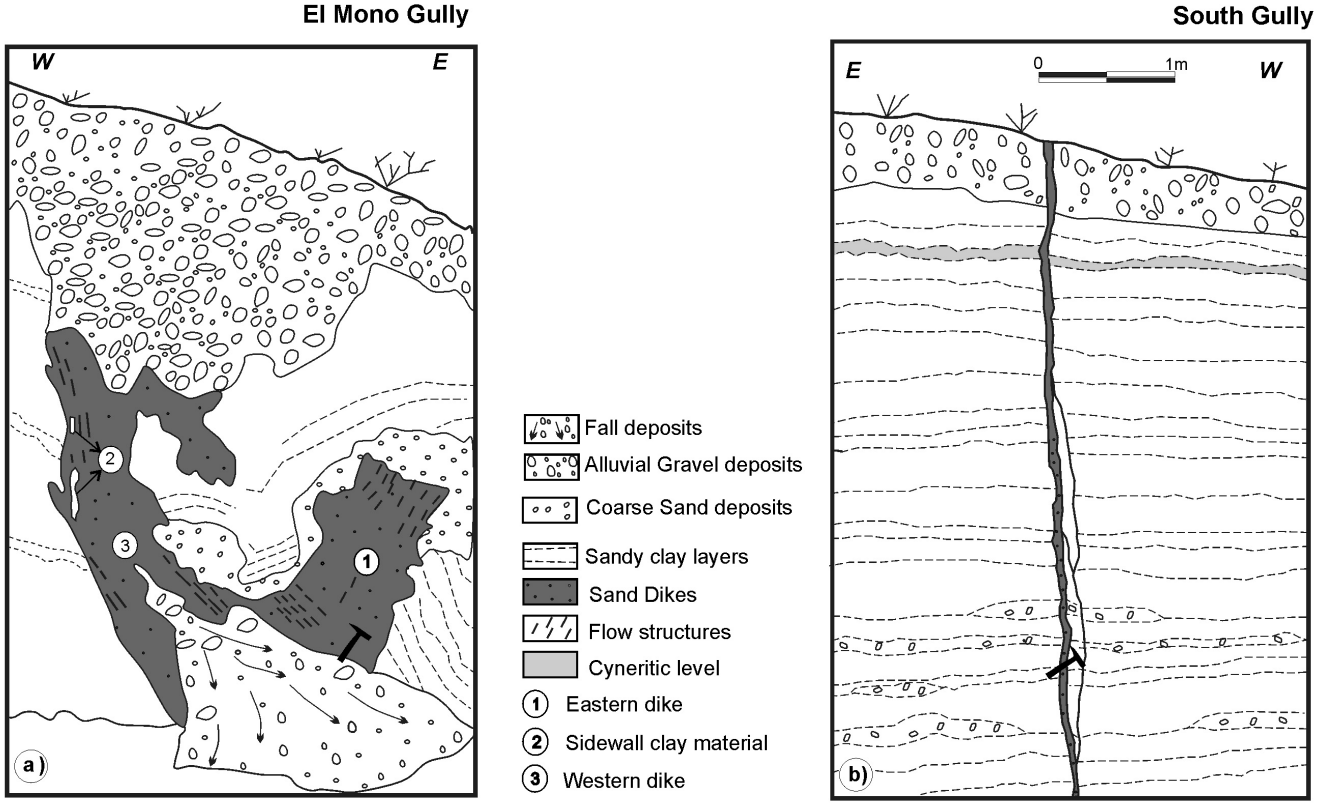

Fig. 8.- a) Scheme of dike with two branches of clastic dikes, the sandy gravel layer and the clay clasts of the sidewall located at the El Mono gully, and b) Narrow dike scheme observed in the South gully (after Paredes and Perucca, 2000).

Fig. 8.- a) esquema del dique con dos ramas de diques clásticos, la capade grava arenosa y los clastos de arcilla del lateral localizado en la quebrada de El Mono, y b) Esquema del dique estrecho observado en la quebrada sur (según Paredes y Perucca, 2000)

$$M = 0.499 \ln (X/3.162x10^{-5}) \quad \text{(eq. 1)}$$

Where (M) is the earthquake moment magnitude and (X) is the maximum epicentral radius in kilometres. Then, Ambraseys (1988) proposed the following equation:

$$M = - 0.31 + (2.65x10^{-8} R_{max}) + (0.99 \log R_{max}) \quad \text{(eq. 2)}$$

Where (M) is the earthquake magnitude moment and (R max) is the maximum epicentral distance from liquefaction in cm. Furthermore, magnitude of the paleoearthquakes related to liquefaction phenomena was also determined in relation with fault length based on Wells and Coppersmith (1994) empirical relationships:

$$M = a + b \times \log (SRL)$$

Where (M) is the earthquake magnitude moment and (SRL) is the surface rupture length, (a) and (b) are coefficient and standard errors.

The length of rupture fault at the surface can be correlated with earthquake magnitude by using the equations proposed by these authors. Estimates of the Moment magnitude of a prehistoric or future earthquake associated with a fault can be made by correlating M with the logarithms of rupture length, that were measured using maps and images.

6. Discussion

Liquefaction features are mainly generated by earthquake shaking (Youd, 1978; Allen, 1975; 1986; Seed 1979, Seed *et al*., 1983). Atkinson (1984) mentioned that earthquake of magnitude 5 can produce liquefaction processes when suitable conditions exist. Nevertheless, similar structures can be created by non-seismic mechanism, for that reason, Obermeier *et al*. (1993) established several conditions required to assign a seismic origin to these structures, such as:

- A strong, sudden hydraulic force directed upwards should be identified.
- Liquefaction features must have characteristics recognizable with historical observations of earthquake-induced liquefaction.
- Sedimentary environment in which the structures originated should be saturated in water.
- Structures must occur at multiple locations in a broad area with similar geologic settings.

All of these conditions could be determined in the study area. Firstly, as was mentioned before, liquefaction phenomena, as well as many landslides, were generated during earthquakes with M >6.3 occurred during the 19th and 20th centuries in San Juan and Mendoza provinces (Bodenbender, 1894; Harrington, 1944; Loos, 1926, 1928; Lünkenheimer, 1929; Perucca and Moreiras, 2006). Furthermore, in the Holocene dammed-lake sequence related to RA-2 rock avalanches, that had to be water saturated, the liquefaction structures were observed in an extensive area. Although slumps are not structures that can be interpreted as seismites per se, their abundance and proximity to the probable seismogenic source may evidence the tectonic instability of the area and a seismic source. Moreover, these structures are also associated with sand dikes and faults which validates our assumption. Examples of pseudo-nodules and dish structures seismically generated have been previously reported by Rodriguez Pascua (1997).

Afterward, at least three triggering paleoearthquakes affected the Holocene lake consistently with the temporal sequence established in the El Mono gully for the called *Oriental, Occidental* and, in the South gully the *Narrow* dike, what was previously noted by Paredes and Perucca (2000). Moreover, it is very likely that the RA-1 and RA-2 rock avalanches had a seismic origin as the occurrence of rock avalanches in the Argentine Andes has been mainly, if not exclusively, related to high magnitude earthquakes (Wayne, 1999; Hermanns *et al*., 2001; Hermanns *et al*., 2005; Moreiras, 2006). This matches with the regional tectonic framework, the presence of Quaternary faults east of the Precordillera Oriental, and the presence of the liquefaction features in paleolakes. For that reason, we presumed that paleoearthquakes affecting this region during Quaternary should be at least 5.

The study of seismites is very important to reconstruct the paleoseismic history of a region determining the seismic nature of the observed features, as well, the magnitude and date of the earthquake (Michetti *et al*., 2005). In this sense, rock avalanches have been widely linked to high magnitude earthquakes (Keefer, 1984, 1987), but they are worst signal of source seismic area because earthquake triggered-landslides can be related to a far epicentre. But, liquefaction features are generally related to close seismic source area so they better signal. The most useful characteristic for determine the probable seismic source area is the width of sand dikes and the size of the associated structures. So, magnitudes of paleoearthquakes can been estimated in other areas by noting the regional extent and size of liquefaction features and comparing these data to known earthquakes in similar settings (Munson *et al*., 1995; Obermeier, 1994; 1998). These authors used this kind of information to arrive at estimates of earthquakes strengths in the Wabash Valley of southern Indiana and Illinois

The field observations reveal that the thickest 4 m-wide sand dikes and the main structures are exposed near the Boca del Acequión in the eastern border of the Holocene lake. At the same time as, the width sand dikes decreases towards the Western border suggesting that the seismogenic source should have been located Eastern of the study area. It is usually assumed that the size and spatial distributions of liquefaction features reflect the location of the source region of a paleoearthquake (Tuttle, 2001). Moreover, the seismogenic source was likely located near from the Acequión river as the width of sand dikes indicates.

Then, knowing the location of the energy centre, the paleoearthquake magnitude can be estimated using the distance to energy centre (Re) (Obermeier and Pond 1999; Obermeier *et al*. 2001). Thus, assuming that liquefaction features in the Acequión region were formed during Holocene activity of the Cerro Salinas fault system, the minimum magnitude of triggering earthquake was estimated independently following equations eq. 1 and eq. 2 established by Allen (1986) and Ambraseys (1988), respectively. According to the former, the minimum magnitude of paleo-earthquakes linked to liquefaction features should have been M>6.6 when considering the maximum distance (Re=18 km) between seismites and the nearest possible seismic source (Cerro Salinas fault). Then, using the equation proposed by Ambraseys (1988), the minimum magnitude of paleoearthquakes results M >5.9. Besides, empirical equations obtain a minimum magnitude ranging Ms 6.3 to Ms 6.7 when Wells and Coppersmith (1994) equations are used.

The empirical relationship between an earthquake magnitude and the distance between the liquefaction structures to the earthquake epicentre has been widely discussed. Seed (1968) determined that M 6 earthquake generates seismites 9 km around the epicentre, while M 7 earthquakes could generate liquefaction structures within a radius of 70 km. Then, Audemard and De Santis (1991) established that liquefaction structures can be found up to 25 km from the epicentre for earthquakes with magnitudes 5 to 5.7. More recently, Obermeier *et al.* (1993) and Moretti *et al.* (1995) noted liquefaction within a 40 km-radius and 100 km-radius from the epicentre generates with M 6 and M 8 earthquakes, respectively. Moreover, the expected maximum distance (Re) can be even greater in some particular cases, such as in the 1977 Caucete earthquake (Ms 7.4) affecting the San Juan province and the north of Mendoza province (Perucca and Moreiras, 2006). In this catastrophic event, liquefaction features

were identified within an area of about 4,000 km^2 and severe damages were observed 260 km far from the epicentre.

Minimum magnitudes estimated by the different empirical methods for paleoearthquakes related to liquefaction structures are consistent. As well, these minimum values are similar to those established by historical records (Ms 6.3) (Perucca and Moreiras, 2006). In addition, rock avalanche occurrence is usually associated with high magnitude earthquakes. According to Keefer (1984, 1987), at least an M 6 earthquake is required to generate such complex landslides. However, we have to consider that magnitudes could be greater if a distant seismogenic area is proposed for paleoearthquakes related to liquefaction structures, as magnitudes estimated empirically in this work are based on assumption of the Cerro Salinas fault system was the seismic source area.

The present study allow to extend to the Holocene the high magnitude paleosismicity of the region as lake liquefacted sediments were dated ca. 7497±157 years ^{14}C BP. Moreover, concluded that seismic source should be the Quaternary Cerro Salinas fault system with recent seismic activity recorded during the earthquakes of 1944 and 1952, and likely to further future reactivations.

7. Conclusions

The identification of earthquake secondary effects along the Acequión river allows to analysed the paleoseismity of the study area.

During historical earthquakes occurred in the region during past 100 years, landslides and liquefaction effects were among the most widespread and most spectacular results of seismic shakes, suggesting that a paleoseismic origin is likely for the two rock avalanches recognized in the area of study.

So, at least five high magnitude paleoearthquakes are estimated through the occurrence of two rock avalanches (RA-1 and RA-2) and the relation of three pulses of liquefaction structures exposed in a paleolake sequence dammed by the younger rock avalanche (RA-2).

Moreover, the Quaternary Cerro Salinas fault zone, N-S trending fault located 20 km from the study area, is suggested as the seismic source of these paleo-earthquakes in accordance with characteristics and distribution of liquefaction features. Then, magnitude of paleoearthquakes is analysed considering minimum magnitude require for triggering identified secondary effects and empirical relations. Earthquakes M >5.5 (epicentral radius less than 25 km) were obtained by the two approaches.

In addition, the Holocene age determined for a basal level of the younger lake related to the liquefaction phenomena, and the correlation of the ash layer overlaying older dammed lake related to RA-1 rock avalanches with previous dated Upper Pleistocene, extend the paleoseismicity to the Quaternary.

Acknowledgements

We thank the reviewers, Juan Rodríguez-Lopez and Pedro Alfaro for thorough reviews, which greatly improved this paper. We are grateful to Dr. Alfonso Sopeña and Dr. Franck Audemard for their helpful comments and advices. This study was supported by CONICET (PID 2163) and CICITCA (21/E 371) from Universidad Nacional de San Juan.

References

Allen, J. (1975): Geologic criteria for evaluating seismicity. *Geological Society of America Bulletin* 86: 1041-1056.

Allen, J. (1986): Earthquake magnitude-frequency, epicentral distance and soft sediment deformation in sedimentary basins. *Sedimentology* 46: 67-75.

Ambraseys, N. (1988): Engineering seismology: earthquake engineering and structural dynamics. *Journal of the International Association of Earthquake Engineering*, 17: 1-105.

Atkinson, G. (1984): Simple computation of liquefaction probability for seismic hazard applications. *Earthquake Spectra*, 1 (1): 107-123.

Audemard, F., De Santis F. (1991): Survey of liquefaction structures induced by recent moderate earthquakes. *Bulletin of the International. Association of Engineering Geology* 44: 5-16.

Bastias, H., Uliarte, E., Paredes, J., Sanchez, A., Bastias, J., Ruzycki, L., Perucca, L. (1990): Neotectónica de la provincia de San Juan. Relatorio de Geología y Recursos Naturales de la provincia de San Juan. *Décimo Primer Congreso Geológico Argentino*, pp. 228-244. San Juan.

Bodenbender, G. (1894): El terremoto argentino. Del 27 de octubre de 1894. *Boletín de la Academia Nacional de Ciencias en Córdoba*. XIV: 293-329.

Costa, C., Machette, M., Dart, R., Bastías, H., Paredes, J., Perucca, L., Tello, G., Haller, K. (2000): Map and Database of Quaternary Faults and Folds in Argentina. *U.S. Geological Survey Open-File Report 00-0108*, 75 p., Denver.

Harrington, H. (1944): El sismo de San Juan del 15 de enero de 1944. C*orporación para la Promoción del Intercambio S.A*. 79 p.

Hermanns, R. L., Niedermann, S., Villanueva García, A., Sosa Gomez, J., Strecker, M.R. (2001): Neotectonics and catastrophic failure of mountain fronts in the southern intra-Andean Puna Plateau, Argentina. *Geology,* 29 (7): 619-623.

Hermanns, R. L., Niedermann, S., Villanueva Gracia A., Schellenberger, A. (2005): Rock avalanching in the NW Argentine Andes as a result of complex interactions of lithologic, structural and topographic boundary conditions, climate change and active tectonics. In: Evans, S. G.; Scarawcia Mugnozza, G.; Strom, A.L. Hermanns, R. L. (Eds.), *Massive rock slope failure.* Proceedings of the NATO Advanced Research Workshop on Massive Rock Slope Failure: New Models for Hazard Assessment*,* Celano, Italy, 16-21 June 2002, Kluwer, 515-539.

INPRES (1993): La verdadera dimensión del problema sísmico en la provincia de San Juan. *Publicación Técnica 18*, San Juan, 46 p.

Jordan, T.E., Gardeweg, M. (1987): Tectonic evolution of the late Cenozoic Central Andes, in: Z. Ben Abraham (Ed.), *Mesozoic and Cenozoic Evolution of the Pacific Margins*, Oxford University Press: 193-207. New York.

Kay, S., Mpodozis, C., Ramos, V., Munizaga, F. (1991). Magma source variations for mid-late Tertiary magmatic rock associated with a shallowing subduction zone and a thickening crust in the central Andes (28º to 33ºS), in: R.S. Harmon, C. W. Rapela (Eds.), Andean Magmatism and its Tectonic Setting. *Geological Society of America Special Paper*, 265: 113-137.

Keefer, D.F. (1984): Landslides caused by earthquakes. *Geological Society of America Bulletin,* 95: 406-21.

Keefer, D.F. (1987): Landslides as indicators of prehistoric earthquakes. Directions in paleoseismology. *U.S. Geological Survey Open File report.* 87-673: 178-180.

Kuribayashi, E.; Tatsuoka, F. (1975): Brief review of liquefaction during earthquakes in Japan. Soils and Foundations, Japan Society Soil Mech. *Found. Eng.,* 15:81-91,

Loos P.A. (1926): Los terremotos del 17 de diciembre de 1920 en Costa de Araujo, Lavalle, La Central, Tres Porteñas, etc. *Contribuciones Geofísicas,* Tomo I, N° 2. Observatorio Astronómico de la Universidad Nacional de La Plata.

Loos P.A. (1928): El terremoto Argentino-Chileno del 14 de abril de 1927. *Contribuciones Geofísicas,* Tomo II, N° 2. Observatorio Astronómico de la Universidad Nacional de La Plata.

Lünkenheimer F. (1929): El terremoto surmendocino del 30 de mayo de 1929. *Contribuciones Geofísicas*, Tomo III, N° 2. Observatorio Astronómico de la Universidad Nacional de La Plata.

Martos, L., (1999): Dinámica morfoestructural del paisaje cuaternario en el piedemonte oriental de la Precordillera Oriental, San Juan. *Décimo Cuarto Congreso Geológico Argentino* Actas, I: 275-278.

Martos, L. (2002). Estimación de máximas magnitudes sísmicas probables del Sistema de Fallamiento Precordillera Oriental, San Juan. *Décimo Quinto Congreso Geológico Argentino*, Actas I: 218-223. Calafate.

Michetti, A.M., Audemard, F.A., Marco, S. (2005): Future trends in paleoseismology: Integrated study of the seismic landscape as a vital tool in seismic hazard analyses. *Tectonophysics,* 408: 3-21.

Moreiras S.M. (2006). Chronology of a Pleistocene rock avalanche probable linked to neotectonic, Cordon del Plata (Central Andes), Mendoza - Argentina. *Quaternary International,* 148: 138-148.

Moretti, M., Pieri, P., Tropeano, M.; Walsh, N. (1995): Tyrrhenian seismites in Bari area (Murge-Apulian foreland). Atti dei Convegni Licenci, 122. *Terremoti in Italia*. Accademia Nazionale dei Lincei: 211 – 216.

Munson, P., Munson, C., Pond, E. (1995): Paleoliquefaction evidence for a strong Holocene earthquake in south-central Indiana. *Geology*, 23: 325-328.

NEIC (2006). USGS National Earthquake Information Center. *On –line catalog*, http://earthquake.usgs.gov/regional/neic/.

Obermeier, S.F. (1994): Using liquefaction-induced features for paleoseismic analysis. In: Obermeier, S., Jibson, W. (Eds.), *Using ground-failure features for paleoseismic analysis. Geological Survey Open-File Report*, 94-633: A1-A98.

Obermeier, S.F. (1996): Use of Liquefaction-induced features for paleoseismic analysis. An overview of how seismic liquefaction features can be distinguished from other features and how their regional distribution and properties can be used to infer the location and strength of Holocene paleo-earthquakes. *Engineering Geology*, 44: 1-76.

Obermeier, S.F. (1998): Liquefaction evidence for strong earthquakes of Holocene and latest Pleistocene ages in the states of Indiana and Ilinois, USA. *Engineering Geology*, 50, 227-254.

Obermeier, S.F., Pond, E.C. (1999): Issues in using liquefaction features for paleoseismic analysis. *Seismological Research Letters*, 70(1), 34-58.

Obermeier, S.F. , Martín, J.R. , Frankel, A.D., Youd, T.L., Munson, C.A., Pond, E.C. (1993): Liquefaction evidence for one or more strong Holocene earthquakes in the Wabash valley of southern Indiana and Illinois, which a preliminary estimate of magnitudes. *U.S. Geological Survey, Professional Paper* 1536, 27 p.

Obermeier, S. F., Pond, E. C., Olson, S.C. (2001): Paleoliquefaction studies in continental settings: geological and geotechnical features in interpretations and back analysis. *U.S. Geological Survey. Open File Report*, 01-29, 75 p.

Ortiz, A., Zambrano, J. (1981): La Provincia Geológica Precordillera Oriental, *Octavo Congreso Geológico Argentino* 3:59-74.

Ortiz, A., Eder, J., Vaca, A. (1975): Evaluación preliminar de las condiciones hidrogeológicas del área Cº Valdivia-Ramblón, Departamento Sarmiento, Provincia de San Juan, Argentina. S*egundo Congreso Ibero-Americano de Geología Económica*, Tomo 3: 75-93. Buenos Aires.

Paredes, J., Perucca, L. (2000): Evidencias de paleolicuefacción en la quebrada del río Acequión, Sarmiento, San Juan. *Revista de la Asociación Geológica Argentina*, 55 (4): 394-397.

Perucca, L.P., Paredes, J.D. (2004): Descripción del Fallamiento activo en la provincia de San Juan. En: *Un volumen de Estudios Sismológicos, Geodésicos y Geológicos en Homenaje al Ingeniero Fernando Séptimo Volponi*. Tópicos de Geociencias. San Juan, 269-309.

Perucca, L.P.; Moreiras, S.M. (2006): Liquefaction phenomena associated with historical earthquakes in San Juan and Mendoza provinces, Argentina. *Quaternary International,* 158: 96-109.

Ramos, V., Cegarra, M., Lo Forte, G., Comínguez, A. (1997): El frente orogénico de la sierra de Pedernal (San Juan, Argentina): su migración a través de los depósitos sinorogénicos. *Actas Octavo Congreso Geológico Chileno*, 3: 1709-1713.

Rodríguez Pascua, M. (1997): Paleosismicidad en emplazamientos nucleares. Estudio en relación con el cálculo de peligrosidad sísmica. Colección Otros Documentos, Consejo de Seguridad Nuclear. Madrid, 286 p.

Seed, H. (1968): Landslides during earthquakes due to solid liquefaction. *American Society of Civil Engineering, Soil Mechanics Foundations Division,* 94: 1053-1122.

Seed, H. (1979): Soil liquefaction and cyclic mobility for level ground during earthquakes: *Journal of Geotechnical Engineering*, 105 (GT2): 201-255.

Seed, H., Idriss, I., Arango, I. (1983): Evaluation of liquefaction potential using field performance data: *Journal of Geotechnical Engineering*, 109 (3): 458-482.

Smalley, R.F., Isacks, B.L. (1990): Seismotectonic of thin and thick-skinned deformation in the Andean foreland from local network data: Evidence for a seismogenic lower crust. *Journal of Geophysical Research*, 95, B8:12487-112498.

Stern, C. (2004): Active Andean volcanism: its geologic and tectonic setting, *Revista Geológica de Chile*, 31(2): 161-206.

Suarez, G., Molnar, P., Burchfield, B.C. (1983): Seismicity, fault plane solutions, depth of faulting and active tectonics of the Andes of Peru, Ecuador and southern Colombia. *Journal of Geophysical Research*, 88: 10403-10428.

Tello, G., Perucca, L. (1993): El Sistema de Fallamiento de Precordillera oriental y su relación con los sismos históricos de 1944 y 1952, San Juan, Argentina. In: *Duodécimo Congreso Geológico Argentino y Segundo Congreso de Exploración de Hidrocarburos*. Actas Tomo III: 246-251. Mendoza.

Tutlle, M. (2001): The use of liquefaction features in paleoseismolo-

gy: Lessons learned in the New Madrid seismic zone, central United States. *Journal of Seismology,* 5: 361-380.

Vergés, J., Ramos, V., Bettini, F., Meigs, A., Cristallini, C., Cortés, J., Dunai, T. (2002): Geometría y edad del anticlinal fallado del cerro Salinas. *Décimo quinto Congreso Geológico Argentino*, Tomo III: 290-294.

Wayne, W.J. (1999): The Alemania rockfall dam: A record of a mid-holocene earthquake and catastrophic flood in northwestern Argentina. *Geomorphology,* 27: 295-306.

Wells, D., Coppersmith, K. (1994): New empirical relationships among magnitude, rupture length, rupture width, rupture area and surface displacement. *Bulletin of the Seismological Society of America,* 84, 974-1002.

Youd, T.L. (1978): Major cause of earthquake damage in ground failure: *Civil Engineering,* 48: 47-51.